Heliyon 10 (2024) e39147

Contents lists available at ScienceDirect

Heliyon

journal homepage: www.cell.com/heliyon

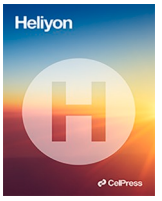

Research article

Preparation and performance of catalyst for organic peroxide wastewater treatment

Zichun Yan [a,b,c,*], Haopeng Ma [c], Mingxia Yang [c]

[a] Ministry of Education Engineering Research Center of Water Resource Comprehensive Utilization in Cold and Arid Regions, Lanzhou, 730070, China
[b] Key Laboratory of Yellow River Water Environment of Gansu Province, Lanzhou, 730070, China
[c] School of Environmental and Municipal Engineering, Lanzhou Jiao Tong University, Lanzhou, 730070, China

ARTICLE INFO

Keywords:
Organic peroxide wastewater
Ozone catalytic oxidation
Cerium dioxide catalyst
Ceramsite
Biodegradability

ABSTRACT

To improve the oxidation pretreatment efficiency of wastewater from organic peroxides, a catalyst (CeO_2-C catalyst) was developed using the calcination method with ceramic particles as the support. The crystalline structure and elemental composition of the CeO_2-C catalyst were characterized by Scanning Electron Microscope (SEM), Energy Dispersive Spectrometer (EDS), and X-ray diffraction (XRD). This study explored the effects of CeO_2 mass ratio, calcination temperature, and calcination time on the performance of the catalyst. The optimal preparation conditions were established through orthogonal experiments. Additionally, the synergistic effect of the catalyst on the ozone oxidation treatment of peroxide wastewater was investigated. The results indicated that the optimal preparation parameters were a CeO_2 mass ratio of 4 %, a calcination temperature of 500 °C, and a duration of 5 h, respectively. After five cycles of reuse, the catalytic activity slightly decreased but remained relatively stable. With an ozone flow rate of 6 L/min, the CeO_2-C/ozone catalytic oxidation process achieved a Chemical Oxygen Demand (COD) removal rate of 28.11 % in wastewater, and the B/C (the ratio of BOD concentration to COD concentration) of wastewater improved from 0.093 to 0.152. The calcination method proved effective for preparing the CeO_2-C catalyst, which demonstrated significant catalytic performance and held promising application prospects in the oxidation pretreatment of organic peroxide wastewater.

1. Introduction

Organic peroxides play a crucial role as crosslinking agents, reaction catalysts, and initiators in the production of plastics, rubber, and resins, significantly contributing to polymer chemical production [1–3]. As industrial enterprises expand, the demand for organic peroxides increases, leading to a rise in the production of wastewater associated with these compounds. This kind of wastewater is characterized by low biodegradability and is challenging to degrade [4–9]. Therefore, wastewater from organic peroxide production typically requires oxidation pretreatment to improve its biodegradability [10–13], and to facilitate the removal of some refractory organic compounds present in the wastewater [14–16]. Common oxidation pretreatment methods include electrocatalytic oxidation,

* Corresponding author. Ministry of Education Engineering Research Center of Water Resource Comprehensive Utilization in Cold and Arid Regions, Lanzhou, 730070, China.
E-mail address: yanzichun@lzjtu.edu.cn (Z. Yan).

https://doi.org/10.1016/j.heliyon.2024.e39147
Received 1 July 2024; Received in revised form 8 October 2024; Accepted 8 October 2024
Available online 9 October 2024

photocatalytic oxidation, ozone catalytic oxidation and so on.

Baral et al. employed copper oxide nanosheets for photocatalytic oxidation technology to degrade organic wastewater. However, the photocatalytic materials currently used in these technologies are nanoscale, making them difficult to recover [17–19]. Jin et al. utilized electrocatalytic oxidation technology to treat urea wastewater [20–22]. However, the high cost, susceptibility to material loss and low current efficiency of electrode materials limit their application in the treatment of high-concentration refractory wastewater. Ozone oxidation alone has problems such as low mineralization of pollutants after treatment, inability to reprocess some organic matter through other means, and low ozone utilization efficiency [38]. Ozone catalytic oxidation reaction can generate · OH with strong oxidation performance, which not only improves the utilization rate of ozone, but also greatly enhances the mineralization and removal rate of pollutants [39]. This technology has developed rapidly in recent years, and many researchers have tended to study and modify ozone catalytic oxidation catalysts [40]. Ozone catalytic oxidation is primarily divided into homogeneous catalysis and heterogeneous catalysis [23,24]. The homogeneous catalytic oxidation system faces issues such as easy loss of active metal ions, low utilization efficiency, high treatment cost, and the potential for secondary water pollution [24–26]. In this study, a heterogeneous CeO_2-C catalyst was prepared using a calcination process, which can be recycled, and maintain stable catalytic activity over a long time without causing secondary pollution [27–29]. The results of this study provide a theoretical basis for the treatment of organic peroxide production wastewater.

2. Materials and methods

2.1. Raw-water quality and measurement method

The water sample for the test was sourced from an auxiliary factory in Gansu Province, specializing in the production of organic peroxides. The primary pollutant in wastewater is organic peroxide. The characteristics of the water quality are detailed in Table 1.

2.2. Test materials

Ceramic particles, serving as the catalyst carriers, featured a specific surface area of 300–1000 m^2, a particle size of 3–5 mm, and a porosity of over 30 %. To adjust the pH of the wastewater, H_2SO_4 and NaOH were employed. Analytical grade HNO_3 and Ce $(NO_3)_3$ were utilized to prepare the catalyst.

2.3. Test device

The schematic diagram of the device is illustrated in Fig. 1. The experiments were carried out within a fume hood, utilizing a 1000 mL conical flask as the reactor for ozone catalytic oxidation. Ozonized air was introduced at the bottom of the conical flask through a dedicated O_3 gas conduit, with the flow of O_3 was controlled by a gas flow meter. Exhaust gas was discharged using a conduit.

2.4. Test methods

2.4.1. Preparation method of catalyst

The cleaned ceramic particles were soaked in HNO_3 solution for 12 h, then filtered, rinsed, dried, and cooled to room temperature. Subsequently, they were immersed in a cerium nitrate solution, thoroughly mixed, and placed on a shaking table for another 12 h. Following this, the particles were filtered and dried in an oven at 105 °C, and then calcined in a Muffle furnace.

2.4.2. Test method for ozone catalytic oxidation

Put 300 mL of test wastewater into a 1000 mL conical flask with a stopper. Adjust the pH with NaOH and dilute H_2SO_4, and conduct the experiment in a fume hood. Connect the aeration head to a conduit, and introduce ozonated air from the bottom of the conical flask using air prepared by the XM ozone disinfection mechanism. Control the flow of ozone using a gas flow meter, and discharge the exhaust gases through a conduit.

2.5. Water quality analysis method

COD concentration was determined by the potassium dichromate colorimetric method. UV_{254} was determined by ultraviolet spectrophotometry, and BOD_5 was measured by the dilution inoculation method. The pH and DO were directly determined by a pHS-25 acidity meter and a HACH HQ-10 dissolved oxygen meter, respectively.

Table 1
Main water quality parameters of wastewater from organic peroxide production.

water quality parameter	COD (mg/L)	BOD_5 (mg/L)	B/C	pH	UV_{254}
Numerical value	12491.3–22493.9	1161.69–2361.86	0.093–0.105	3.83–6.35	2.312–3.550

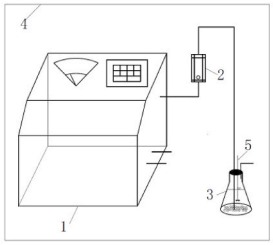

1 - ozone generator; 2-gas flowmeter; 3-conical flask; 4-fume hood;5-Magnetic stirrer

Fig. 1. Schematic diagram of ozone catalytic oxidation test device.

3. Results and discussion

3.1. Optimization of catalyst preparation conditions

The catalytic properties of cerium [30], cobalt [31], and manganese ions [32] were systematically investigated. Three distinct catalysts were synthesized under the same experimental conditions, which included an ozone flux rate of 5 L/min, an initial solution pH of 6, and a reaction duration of 60 min. This study explored the influence of varying elemental loadings on the efficiency of pollutant removal when using ceramic particles as carriers. The comparative performance of these catalysts is illustrated in Fig. 2.

The removal rates of COD and UV_{254} from wastewater by three catalysts in the ozone catalytic oxidation experiments were 26.12 %, 24.30 %, 24.06 % for COD and 22.37 %, 20.93 %, 20.74 % for UV_{254}, respectively. Among them, the CeO_2 catalyst exhibited superior performance. This enhanced efficacy can be attributed to the semi-open fluorite structure of CeO_2 crystals, which uniquely enables the release of oxygen in oxygen-deficient environments and the storage of oxygen in oxygen-rich environments (Kim et al., 2023; A. Wang et al., 2023). Additionally, the CeO_2 lattice features high oxygen mobility (Guo et al., 2022; Zhou et al., 2024).

3.2. Optimization of preparation conditions of CeO_2-C catalyst

To obtain the specific level values for each factor in the orthogonal experiment, the influence of various preparation conditions on the performance of the catalyst were initially investigated by single-factor experiments. Subsequently, the optimal preparation conditions for the catalyst were determined by an orthogonal experiment.

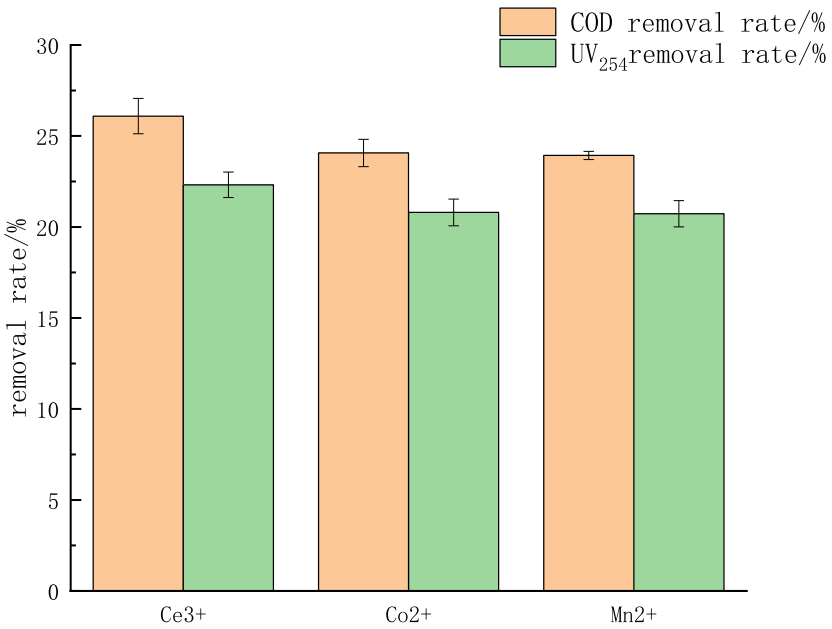

Fig. 2. Optimization of active components.

3.2.1. Single-factor experiment

3.2.1.1. The influence of CeO_2 mass ratio on pollutant removal rate. During the preparation of CeO_2-C catalyst, the effect of different CeO_2 mass ratios on the catalyst performance was investigated. Under this experimental condition, the COD concentration of raw water was measured at 22102.7 mg/L, and the UV_{254} value was 3.354.

As depicted in Fig. 3, as the mass fraction of CeO_2 on ceramic particles increases from 2 % to 10 %, the removal rates of COD and UV_{254} in wastewater by ozone catalytic oxidation exhibited a trend of initially increasing and then decreasing. The removal rates peaked at a CeO_2 mass fraction of 4 %, achieving 25.86 % for COD and 19.55 % for UV_{254}, respectively. In the reaction system, · OH can be catalyzed by the active sites on the catalyst to produce ozone. An increase in CeO_2 loading can increase the amount of · OH in the system, improving the removal rate of pollutants. However, when the loading is too large, it can block some of the pores of the catalyst, resulting in a decrease in the effectiveness of ozone catalytic oxidation [41]. These results indicating that the optimal CeO_2 mass ratio is 4 %.

3.2.1.2. Effect of calcination temperature on pollutant removal rate. In the process of preparing CeO_2-C catalyst, the effects of different calcination temperatures (300 °C, 400 °C, 500 °C, 600 °C, 700 °C) on the performance of catalyst were investigated. The experiments maintained a fixed CeO_2 loading of 4 % and a calcination duration of 4 h. Under these conditions, the COD concentration of the raw water was 21924.7 mg/L, and the UV_{254} value was 3.493.

As illustrated in Fig. 4, the removal rates of COD and UV_{254} from wastewater via ozone catalytic oxidation demonstrate a trend of increasing and then decreasing as the calcination temperature rises from 300 °C to 700 °C. At lower temperatures, the nitrate on the ceramsite can not be fully decomposed [33], resulting in a lower catalytic effect. As the temperature gradually increases, the carrier generates more basic groups and active sites, thus improving the performance of the catalyst. However, at excessively high temperatures, the pore structure of the catalyst is compromised, resulting in a decrease in catalyst activity [34]. The optimal calcination temperature obtained through comparison is 500 °C.

3.2.1.3. Effect of calcination time on pollutant removal rate. During the preparation of the CeO_2-C catalyst, the calcination CeO_2 loading was controlled at 4 %, and the calcination temperature was 500 °C. The influence of different calcination durations (2, 3, 4, 5 and 6 h) on the performance of the catalyst was investigated. Under this condition, the COD concentration of raw water was 22137.5 mg/L, and the UV_{254} value was 3.427.

As depicted in Fig. 5, the removal rates of COD and UV254 in the ozone catalytic oxidation experiments demonstrate distinct trends with varying calcination durations from 2 h to 6 h. The rates for COD were 18.44 %, 22.75 %, 23.21 %, 25.89 %, 23.7 %, and for UV_{254}, they were 16.97 %, 17.79 %, 18.57 %, 20.24 % and 19.19 %, respectively. These trends indicate an initial increase followed by a decrease in removal efficacy. At a calcination time of 5 h, both COD and UV_{254} achieve their peak removal rates, recorded at 25.89 % and 25.24 %, respectively. The formation of active oxide crystals within the catalysts is a relatively slow process, significantly influenced by the duration of the calcination [35]. Insufficient calcination times fail to completely decompose the cerium nitrate active

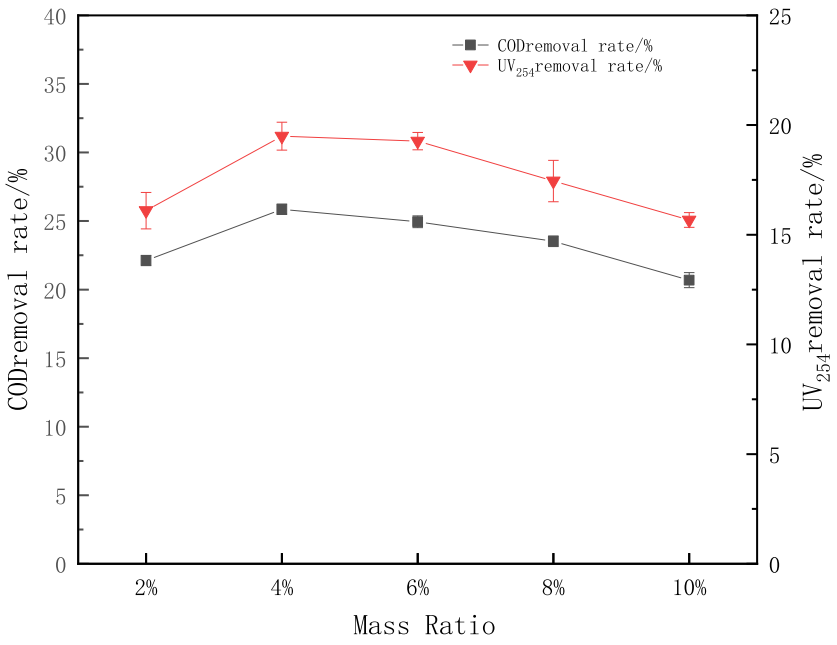

Fig. 3. Effect of CeO_2 loading on pollutant removal rate.

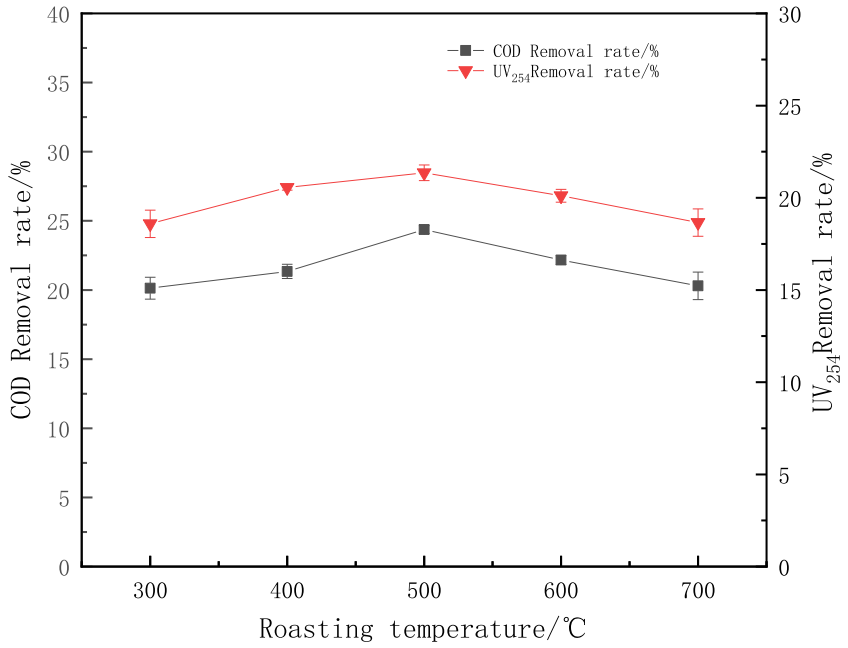

Fig. 4. Effect of calcination temperature on pollutant removal rate.

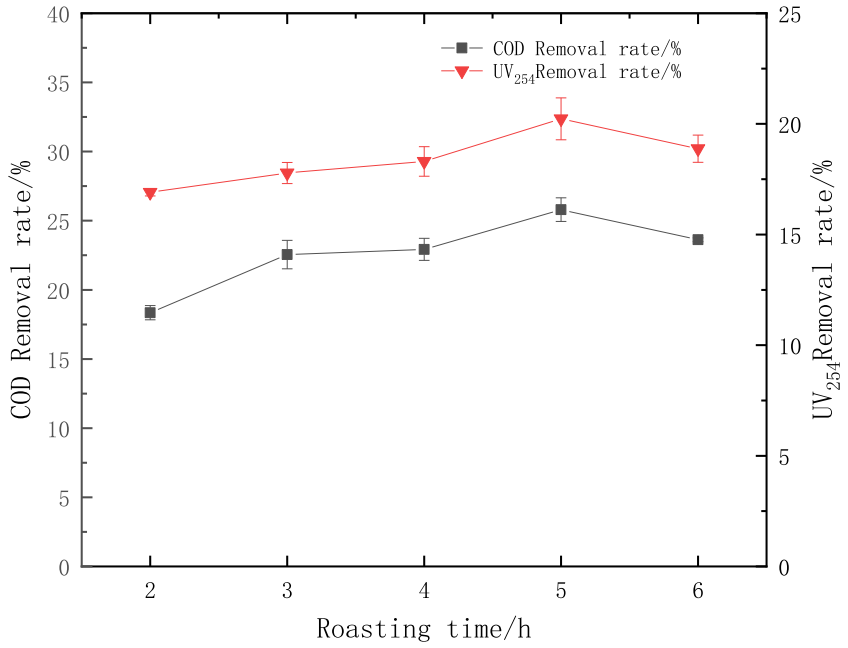

Fig. 5. Effect of calcination duration on pollutant removal rate.

components, thereby limiting the catalytic effectiveness. Conversely, excessively prolonged calcination leads to structural degradation of the catalyst's porous network, diminishing its catalytic capabilities [36]. In conclusion, the optimal calcination period, ensuring maximum catalytic activity is established at 5 h.

3.2.2. Optimization of CeO_2-C catalyst preparation by orthogonal testing

The preparation process of the CeO_2-C catalyst was further optimized by an orthogonal testing methodology. Three factors variables were considered in this optimization: CeO_2 mass ratio, calcination temperature (°C) and calcination duration (H). The removal rate of COD was employed as the metric to assess the catalytic activity of the catalyst. The concentration of COD in the raw water used

for this test was 22,093.6 mg/L. The levels of each factor are encoded in Table 2.

To further analyze the impact of various factors on COD removal efficiency, a range of analyses were conducted based on the COD removal rate results presented in Tables 2 and 3. The outcomes of this analysis are shown in Table 4.

In Table 4, the order of factors affecting the performance of the CeO_2 catalyst is as follows: CeO_2 mass ratio > calcination temperature > calcination time, with the CeO_2 mass ratio having the most significant influence. Under the optimal experimental conditions ($A_2B_2C_2$), the prepared catalyst was applied in the ozone catalytic oxidation experiment, achieving a COD removal rate of 24.71 %.

3.2.3. Catalyst stability

The CeO_2-C catalyst, prepared under the optimal conditions determined by both single factor and orthogonal tests, and was applied in ozone catalytic oxidation experiments to investigate its stability. Under these conditions, the COD concentration of the raw water was 22281.9 mg/L, and the UV_{254} value was 3.399.

As shown in Fig. 6, when the number of use of catalysts used increased from 1 to 5, the removal rate of pollutants exhibited a downward trend. The removal rates for COD were 24.07 %, 23.52 %, 23.98 %, 22.01 %, 21.49 %, while the UV_{254} removal rates were 20.29 %, 19.09 %, 19.66 %, 18.56 % and 18.41 %, respectively. Over the course of five reuse tests, the COD and UV254 removal rates remained between 20 %–25 % and 18 %–21 %. In general, CeO_2-C catalyst demonstrated good stability, which could be attributed to the secure loading of CeO_2 on the ceramic particles, preventing significant loss of the active component [37].

3.3. Characterization of catalysts

The morphology and structure of CeO_2-C catalyst were characterized by scanning electron microscope (SEM), energy dispersive spectrometer (EDS) and X-ray diffraction (XRD).

(1) The SEM characterization analysis of the original ceramsite and loaded ceramsite is shown in Fig. 7.

From Fig. 7 (a), it is evident that the surface of ceramic particles is rough and uneven, a characteristic that facilitates the loading of metals and metal oxides. From Fig. 7 (b), a large number of nanoscale particles can be observed attached to the surface of ceramic particles.

(2) EDS

The EDS characterization analysis of the original ceramsite and loaded ceramsite is shown in Fig. 8.

As shown in Fig. 8, the ceramic particles are primarily composed of Ca, O, Mg, Al, Si, K, Fe, and other elements. After the loading process, the surface of the ceramic particles contains Ce element, indicating that cerium metal and its oxides have been successfully deposited onto the ceramic particles.

(3) XRD

As shown in Fig. 9, the diffraction peaks of the catalyst CeO_2-C prepared by the loading method match the standard spectrum of CeO_2, clearly indicating that CeO_2 crystals have successfully formed on the ceramsite.

3.4. CeO_2-C ozone catalytic oxidation test

(1) Influence of catalyst dosage on treatment effect

As depicted in Fig. 10, when the dosage of CeO_2-C increases from 5 g/L to 30 g/L, the removal rates of COD and UV_{254} demonstrate a trend of initial rise, followed by a slight decline. At a catalyst dosage of 25 g/L, the removal rates of COD and UV254 increase by only 0.96 % and 0.35 %, respectively, compared to a dosage of 20 g/L. This small improvement suggests that increasing the dosage beyond 20 g/L leads to inefficient use of the catalyst and some level of wastage. Based on this analysis, the optimal dosage of CeO2-C was determined to be 20 g/L for effective pollutant removal.

The reason for the analysis is that increasing the dosage of CeO2-C in the system gradually increases the number of active sites provided for the reaction system, thus improving the catalytic oxidation treatment effect. However, when it exceeds a certain amount, it will cause agglomeration and result in a decrease in treatment effectiveness [42,43].

Table 2
Orthogonal test factors and level design.

Variable	Code	Level value		
CeO_2 Mass proportion	A	2 %	4 %	6 %
calcination temperature	B	400	500	600
calcination time	C	4	5	6

Table 3
Operation results of orthogonal test.

Serial Number	Factor			COD removal rates/%
	A	B	C	
1	2	400	4	21.26
2	2	500	5	22.30
3	2	600	6	19.06
4	4	400	5	23.18
5	4	500	6	24.30
6	4	600	4	22.36
7	6	400	6	20.38
8	6	500	4	21.68
9	6	600	5	21.39

Table 4
The results of COD range analysis.

Project	Factor		
	A	B	C
K1	20.87	21.61	21.77
K2	23.28	22.76	22.29
K3	21.15	20.94	21.25
Range	2.13	1.82	1.04
optimal level	A_2	B_2	C_2
Factor priority		A > B > C	
Optimal combination		$A_2B_2C_2$	

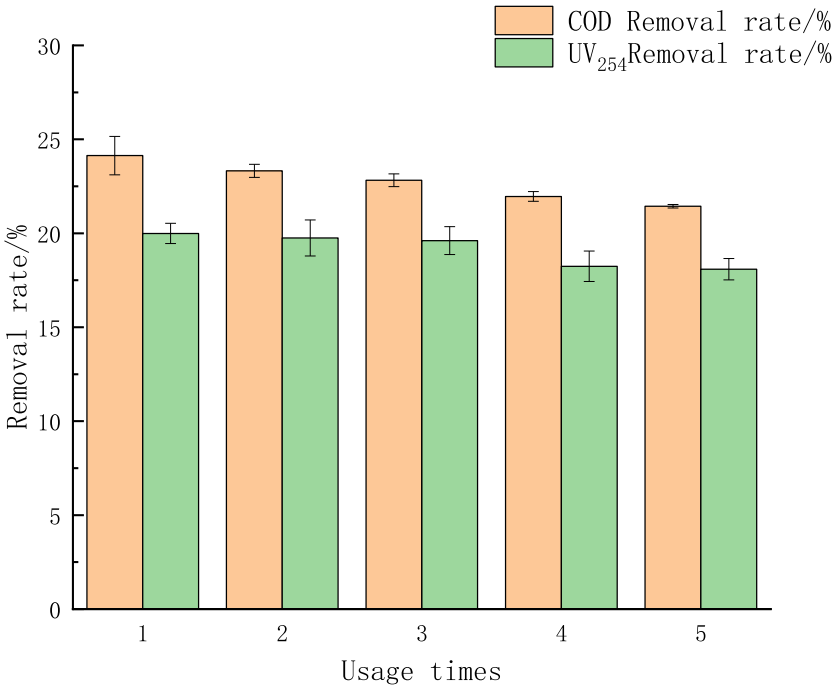

Fig. 6. Stability of the catalyst.

(2) Effect of reaction time on treatment effect

As illustrated in Fig. 11, extending the reaction time of ozone catalytic oxidation from 15 min to 120 min results in a gradual increase in the removal rates of COD and UV_{254}. Before reaching a reaction time of 60 min, the removal rates of wastewater pollutants increase rapidly with time. Beyond 60 min, the COD removal rate continues to increase, but the growth rate of improvement slows significantly, while the UV_{254} removal rate shows minimal further change. The reason may be that when the reaction time reaches 60

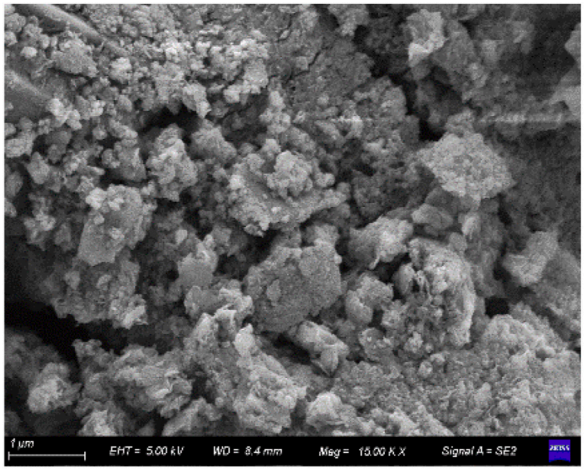

a （Protoceramsite）

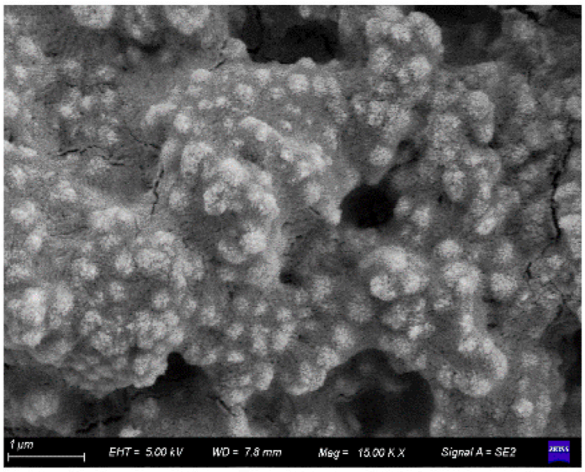

b （Ceramsite after loading）

Fig. 7. SEM images of original ceramsite and loaded ceramsite.

min, the · OH generated by catalytic ozone oxidizes all organic matter such as humus and aromatic compounds that can be oxidized in the wastewater. Therefore, the removal rate of UV_{254} in the wastewater no longer increases, and other organic matter continues to be oxidized, resulting in a slow increase in COD removal rate [44]. Based on these observations, the optimal reaction time for effective pollutant removal is determined to be 60 min.

(3) Biodegradability of wastewater treated by CeO_2-C ozone catalytic oxidation

Under the experimental conditions of an ozone flow rate of 6 L/min, a CeO_2-C catalyst dosage of 20 g/L, a solution pH of 6, and a reaction time of 60 min, the COD concentration of the wastewater after CeO_2-C ozone catalytic oxidation pretreatment was reduced to 16067.7 mg/L, while the BOD_5 concentration increased to 2441.3 mg/L. Consequently, the B/C ratio of the treated wastewater improved to 0.152, indicating enhanced biodegradability. The reason for this is that ozone can oxidize complex organic compounds such as polycyclic aromatic hydrocarbons in wastewater into substances that are easily utilized by microorganisms. Ozone catalytic oxidation not only improves the utilization rate of ozone and the mineralization of pollutants, but also degrades more complex organic compounds into small molecule substances that are easily utilized by microorganisms. Therefore, CeO2-C ozone catalytic oxidation pretreatment technology significantly improves the biodegradability of wastewater [45].

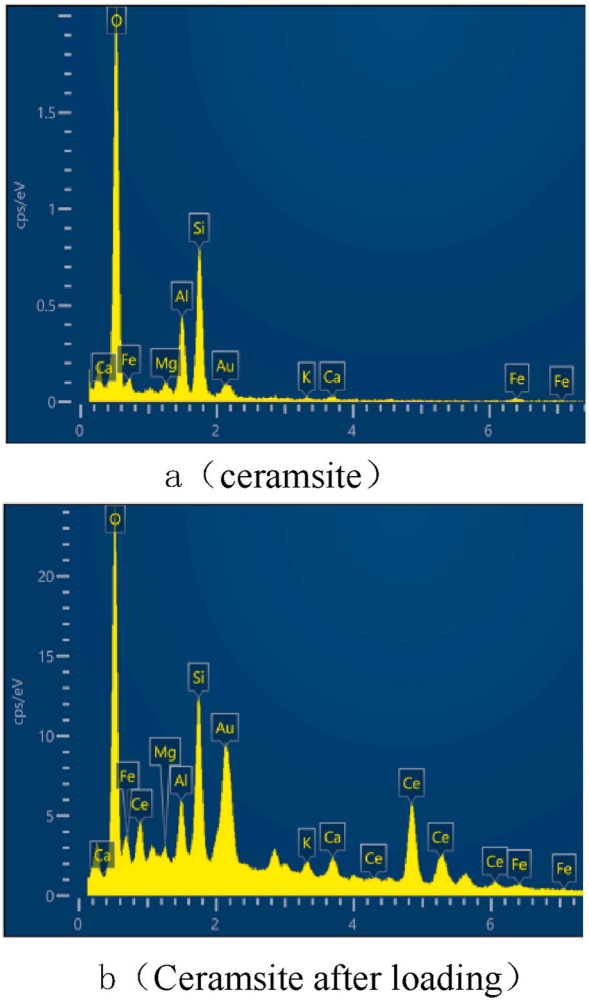

Fig. 8. EDS spectra of raw ceramsite and loaded ceramsite.

4. Conclusion

(1) Taking the COD removal rate as the evaluation index, orthogonal experiments were conducted to optimize the preparation conditions of the CeO_2 catalyst. The order of influencing factors was determined to be CeO_2 mass ratio > calcination temperature > calcination time. The catalyst prepared under the conditions of a 4 % CeO_2 mass ratio, a calcination temperature of 500 °C, and a calcination time of 5 h exhibited superior performance.

(2) SEM analysis revealed that the surface of ceramic particles was rough, which promotes the effective loading of active components. EDS indicates that cerium metal or its oxide was successfully deposited on the surface of the ceramic particles, while XRD indicates that the metal oxide on the catalyst surface was CeO_2 crystals.

(3) The CeO_2-C catalyst prepared under the optimal conditions, when used in conjunction with ozone for catalytic oxidation, achieved COD and UV_{254} removal rates of 28.11 % and 21.75 %, respectively. Furthermore, the B/C ratio of wastewater increased from 0.093 to 0.152, indicating a significant improvement in the biodegradability of the wastewater.

CRediT authorship contribution statement

Zichun Yan: Writing – review & editing, Supervision, Project administration, Methodology, Funding acquisition. **Haopeng Ma:** Writing – review & editing, Writing – original draft. **Mingxia Yang:** Visualization, Validation, Methodology, Data curation, Conceptualization.

Data availability

All data generated or analyzed during this study are included in this article.

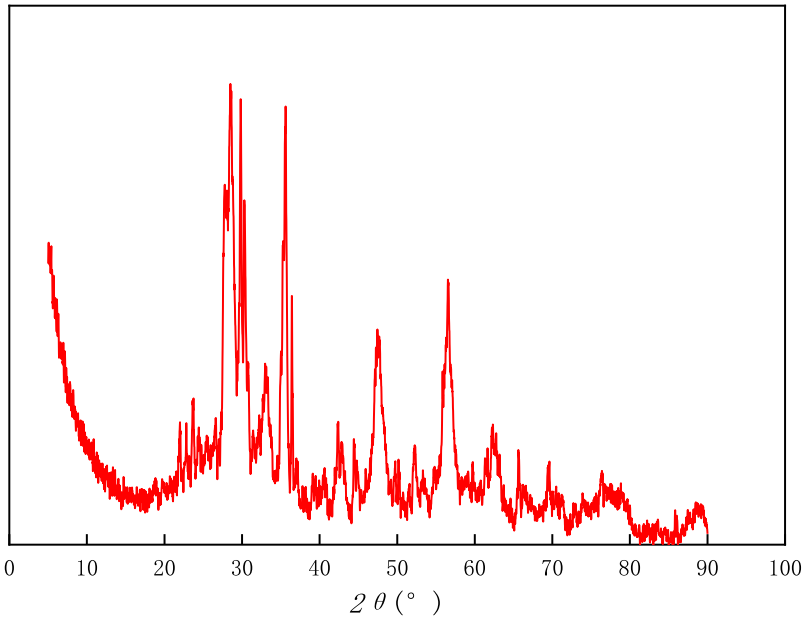

Fig. 9. XRD spectrum of CeO_2-C catalyst.

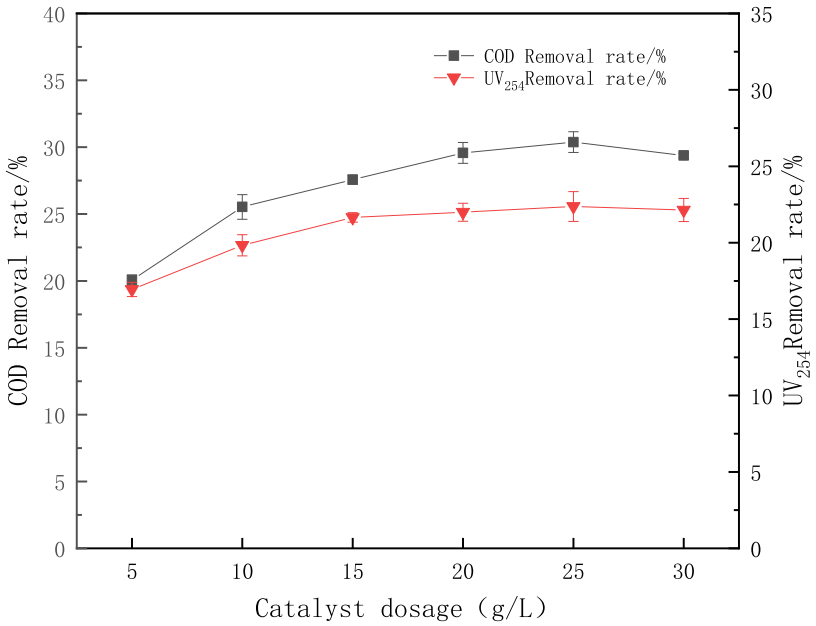

Fig. 10. Effect of catalyst dosage on pollutant removal rate.

Ethics approval and consent to participate

Not applicable.

Consent for publication

Not applicable.

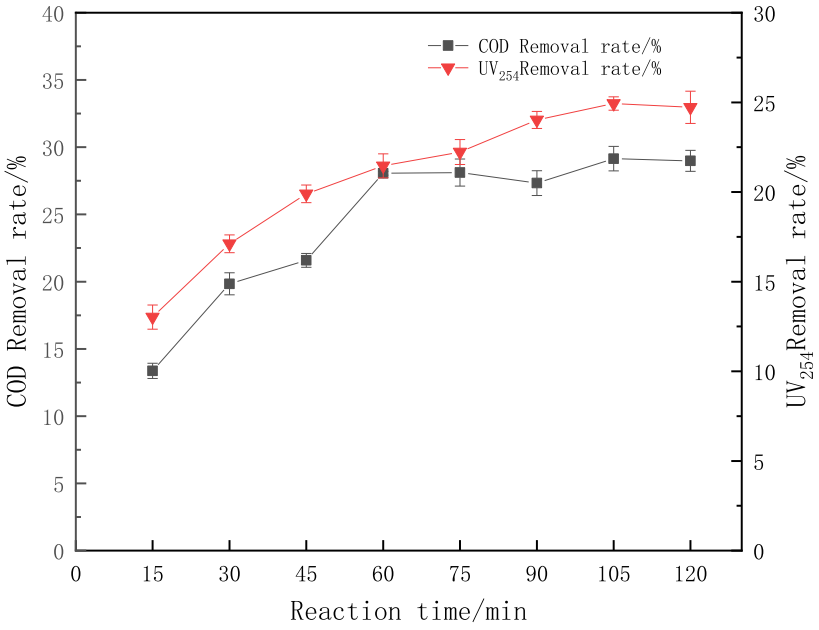

Fig. 11. Effect of reaction time on pollutant removal rate.

Funding

The research was supported by the Open Foundation of Key Laboratory of Yellow River Water Environment in Gansu Province (20JR2RA0002), and the National Natural Science Foundation of China (51568034).

Declaration of competing interest

The authors declare that they have no known competing financial interests or personal relationships that could have appeared to influence the work reported in this paper.

Acknowledgments

The authors would like to acknowledge/thank the heads of the fund project.

References

[1] C. Liu, Y. Chu, R. Wang, J. Fan, Preparation of lotus-leaf-like carbon cathode for the electro-Fenton oxidation process: hydrogen peroxide production, various organics degradation and printing wastewater treatment, J. Water Process Eng. 52 (2023) 103596.
[2] C.-D. Dong, J.-W. Cheng, C.-W. Chen, C.-P. Huang, C.-M. Hung, Activation of calcium peroxide by nitrogen and sulfur co-doped metal-free lignin biochar for enhancing the removal of emerging organic contaminants from waste activated sludge, Bioresour. Technol. 374 (2023) 128768.
[3] P. Chen, M. Zhou, Y. Liu, B. Li, C. Chen, X. Duan, Y. Wang, Carbon nitride in peroxide-coupled photocatalysis for aqueous organic pollutants destruction: engineered active sites and electron transfer regimes, Appl. Catal., B: Environment and Energy 346 (2024) 123767.
[4] A. Baraka, M. Sheashea, K. Gado, O. Abuzalat, Cerium-phthalate coordination polymer as fenton-like durable catalyst for hydrogen peroxide activation and anionic organic dyes degradation in wastewater, Mater. Sci. Eng., B 297 (2023) 116801.
[5] V.L.N. Vo, T.-T. Luu, Y.-M. Chung, Catalytic wet peroxide oxidation with in-situ generated H2O2: an efficient strategy for improving the stability of metal-organic framework catalysts, Catal. Today 425 (2024) 114316.
[6] M. Pinz, L. Felipe de Souza, D. Vileigas, B. Dempsey, I. Medeiros, L. Diniz, N. Oddone, G. Ferrer-Sueta, S. Miyamoto, M. Comini, F. Meotti, Characterization of a fluorescent biosensor with specificity for organic peroxides, Free Radic. Biol. Med. 208 (2023) S136.
[7] A. Ruiz-Sánchez, G.T. Lapidus, Decomposition of organic additives in the oxidative chalcopyrite leaching with hydrogen peroxide, Miner. Eng. 187 (2022) 107783.
[8] T. Chongcharoenchaikul, K. Miyaji, P. Junkong, S. Poompradub, Y. Ikeda, Effects of organic components in cuttlebone on the morphological and mechanical properties of peroxide cross-linked cuttlebone/natural rubber composites††Electronic supplementary information (ESI), RSC Adv. 12 (2022) 13557–13565, https://doi.org/10.1039/d2ra01885c, available. See.
[9] G. Varank, S. Yazici Guvenc, E. Can-Güven, S. Yokus, O.N. Bilgin, Hydrogen peroxide assisted advanced electrocoagulation for reducing the organic content of leachate nanofiltration concentrate, J. Ind. Eng. Chem. 132 (2024) 369–382.
[10] Y. Zhao, Y. Wang, H. Chi, Y. Zhang, C. Sun, H. Wei, R. Li, Coupling photocatalytic water oxidation on decahedron BiVO4 crystals with catalytic wet peroxide oxidation for removing organic pollution in wastewater, Appl. Catal. B Environ. 318 (2022) 121858.
[11] G. Ning, Q. Duan, H. Liang, H. Liu, M. Zhou, C. Chen, C. Zhang, H. Zhao, C. Li, One stone two birds: electrochemical and colorimetric dual-mode biosensor based on copper peroxide/covalent organic framework nanocomposite for ultrasensentive norovirus detection, Food Sci. Hum. Wellness 13 (2024) 920–931.

[12] H. Wang, C. Li, T. Li, M. Yang, Photoelectrochemical detection of circulation tumor cell based on metal-organic framework with incorporated copper peroxide nanodots as probe, Mater. Lett. 361 (2024) 136090.
[13] F. Wang, L. Liao, X. Liu, J. Zhang, F. Wu, Porphyrin-based porous organic frameworks as efficient peroxidase mimics for selective detection of hydrogen peroxide and glucose, Inorg. Chem. Commun. 155 (2023) 111011.
[14] A.R. Dinçer, D.İ. Çifçi, D.D. Cinkaya, E. Dülger, F. Karaca, Treatment of organic peroxide containing wastewater and water recovery by fenton-adsorption and fenton-nanofiltration processes, J. Environ. Manag. 299 (2021) 113557.
[15] L.-Q. Gong, L. Li, Y. Pan, J.-J. Jiang, J.-C. Jiang, Thermal hazards and initial decomposition mechanisms study of four tert-butyl organic peroxides combining experiments with density functional theory method, Thermochim. Acta 708 (2022) 179142.
[16] F. Chen, W. Ren, X. Liu, Y. Zhao, Q. Guo, C. Lin, M. He, W. Ouyang, Synergistic removal of organic and inorganic composite pollutants from water by zero-valent iron activated calcium peroxide, Chem. Eng. J. 476 (2023) 146919.
[17] S.C. Baral, P. Maneesha, S. Datta, K. Dukiya, D. Sasmal, K.S. Samantaray, V.K. Br, A. Dasgupta, S. Sen, Enhanced photocatalytic degradation of organic pollutants in water using copper oxide (CuO) nanosheets for environmental application, JCIS Open 13 (2024) 100102.
[18] Y. Chen, D. Zhu, S. Xue, H. Wang, Q. Lu, G. Ruan, C. Zhao, F. Du, Construction of S-scheme BiOCl/layered bimetallic oxide heterojunction for enhanced photocatalytic degradation of bisphenol A, Appl. Surf. Sci. 653 (2024) 159337.
[19] R. Li, C. Zhang, K. You, B. Li, W. Bu, X. Meng, B. Ma, Y. Ding, Molecular confined synthesis of magnetic CoOx/Co/C hybrid catalyst for photocatalytic water oxidation and CO2 reduction, Chin. Chem. Lett. 34 (2023) 108801.
[20] J. Jin, L. Zhou, W. Sun, Y. Zheng, B. Liu, Study on the electrocatalytic oxidation of urea at nickel/iron deposited electrodes, Int. J. Electrochem. Sci. 18 (2023) 100318.
[21] Q. Huang, L. Dai, S. Zhang, P. Hu, L. Ci, Optimization effect of Ag-regulated manganese oxides on electrocatalytic performance for Li–O2 batteries††Electronic supplementary information (ESI) available. See, Catal. Sci. Technol. 13 (2023) 6792–6798, https://doi.org/10.1039/d3cy00830d.
[22] J. Rozendo, M.A.S. Garcia, S.L.S. Lima, N. Tasić, B. Emrem, J.L. Fiorio, G. Solorzano, A.H.B. Dourado, L.M. Gonçalves, T.R.L.C. Paixão, J.-O. Joswig, A.G.M. da Silva, P. Vidinha, How do gold-nanocrystal surface facets affect their electrocatalytic activities and the benzocaine-oxidation mechanism? Surface. Interfac. 41 (2023) 103282.
[23] K.-C. Chen, Y.-H. Wang, The effects of Fe–Mn oxide and TiO2/α-Al2O3 on the formation of disinfection by-products in catalytic ozonation, Chem. Eng. J. 253 (2014) 84–92.
[24] S. Dong, W. Xu, Q. Guo, K. Luo, H. Cheng, J. Tang, D. Wang, Z. He, L. Wang, S. Song, J. Ma, Enhanced 2, 6-dimethylpyrazine removal by catalytic ozonation with legumes biochar: the roles of oxygen- and nitrogen-containing functional groups, Sep. Purif. Technol. 334 (2024) 125991.
[25] M.-H. Yuan, C.-Y. Chang, J.-L. Shie, C.-C. Chang, J.-H. Chen, W.-T. Tsai, Destruction of naphthalene via ozone-catalytic oxidation process over Pt/Al2O3 catalyst, J. Hazard Mater. 175 (2010) 809–815.
[26] L. Fu, P. Wang, C. Wu, Y. Zhou, Y. Song, S. Guo, Z. Li, J. Zhou, Upgrade of the biggest catalytic ozonation wastewater treatment plant in China: from pollution control to carbon reduction, J. Environ. Manag. 349 (2024) 119421.
[27] H. Zhuang, H. Han, B. Hou, S. Jia, Q. Zhao, Heterogeneous catalytic ozonation of biologically pretreated Lurgi coal gasification wastewater using sewage sludge based activated carbon supported manganese and ferric oxides as catalysts, Bioresour. Technol. 166 (2014) 178–186.
[28] L. Jothinathan, J. Hu, Kinetic evaluation of graphene oxide based heterogenous catalytic ozonation for the removal of ibuprofen, Water Res. 134 (2018) 63–73.
[29] X. Li, J. Ma, C. Zhang, R. Zhang, H. He, Facile synthesis of Ag-modified manganese oxide for effective catalytic ozone decomposition, J. Environ. Sci. 80 (2019) 159–168.
[30] C.A. Orge, J.J.M. Órfão, M.F.R. Pereira, Catalytic ozonation of organic pollutants in the presence of cerium oxide–carbon composites, Appl. Catal. B Environ. 102 (2011) 539–546.
[31] E. Zhang, P. Zhao, G. Xu, F. Meng, X. Wang, Y. Gao, L. Liu, S. Jin, High efficiency manganese cobalt spinel structure catalytic ozonation ceramic membrane for in situ BPA degradation and membrane fouling elimination, J. Environ. Chem. Eng. 12 (2024) 111774.
[32] A. Xu, S. Fan, T. Meng, R. Zhang, Y. Zhang, S. Pan, Y. Zhang, Catalytic ozonation with biogenic Fe-Mn-Co oxides: biosynthesis protocol and catalytic performance, Appl. Catal. B Environ. 318 (2022) 121833.
[33] C. Chen, X. Yan, B.A. Yoza, T. Zhou, Y. Li, Y. Zhan, Q. Wang, Q.X. Li, Efficiencies and mechanisms of ZSM5 zeolites loaded with cerium, iron, or manganese oxides for catalytic ozonation of nitrobenzene in water, Sci. Total Environ. 612 (2018) 1424–1432.
[34] C. Shan, Y. Xu, M. Hua, M. Gu, Z. Yang, P. Wang, Z. Lu, W. Zhang, B. Pan, Mesoporous Ce-Ti-Zr ternary oxide millispheres for efficient catalytic ozonation in bubble column, Chem. Eng. J. 338 (2018) 261–270.
[35] J. Restivo, C.A. Orge, A.S.G.G. Santos, O.S.G.P. Soares, M.F.R. Pereira, Nano- and macro-structured cerium oxide – carbon nanotubes composites for the catalytic ozonation of organic pollutants in water, Catal. Today 384–386 (2022) 187–196.
[36] N.P. Chokshi, A. Chauhan, R. Chhayani, S. Sharma, J.P. Ruparelia, Preparation and application of Ag–Ce–O composite metal oxide catalyst in catalytic ozonation for elimination of Reactive Black 5 dye from aqueous media, Water Sci. Eng. (2023).
[37] Y. Zhang, M. Chen, Z. Zhang, Z. Jiang, W. Shangguan, H. Einaga, Simultaneously catalytic decomposition of formaldehyde and ozone over manganese cerium oxides at room temperature: promotional effect of relative humidity on the MnCeOx solid solution, Catal. Today 327 (2019) 323–333.
[38] X. Chen, C. Zhou, Q. Ke, Y. Zhou, X. Zeng, Z. Jin, H. Liu, H. Lu, Ethanol-thermal synthesis of colloidal-CeFeMn mixed-oxide as efficient catalytic material for atmospheric ozone decomposition, Colloids Surf. A Physicochem. Eng. Asp. 676 (2023) 132238.
[39] N.P. Chokshi, A. Chauhan, R. Chhayani, S. Sharma, J.P. Ruparelia, Preparation and application of Ag–Ce–O composite metal oxide catalyst in catalytic ozonation for elimination of Reactive Black 5 dye from aqueous media, Water Sci. Eng. 17 (2024) 257–265.
[40] L. Liang, P. Cao, X. Qin, S. Wu, H. Bai, S. Chen, H. Yu, Y. Su, X. Quan, Oxygen vacancies-driven nonradical oxidation pathway of catalytic ozonation for efficient water decontamination, Appl. Catal. B Environ. 325 (2023) 122321.
[41] L. Ma, C. Miao, P. Ma, G. Guo, B. Yang, L. Li, Y. Liu, B. Lai, Pretreatment of shale gas flowback water (SGFW) by hydroxylamine and FexOy/γ-Al2O3 synergistic catalytic ozone oxidation (HSCO), J. Water Process Eng. 59 (2024) 104972.
[42] A. Wang, H. Zhao, Y. Wu, Q. Zhang, C. Han, Cerium-modified amorphous manganese oxides for efficient catalytic removal of ozone, J. Environ. Sci. 131 (2023) 151–161.
[43] Y. Yuan, J. Liu, B. Gao, J. Hao, Ozone direct oxidation pretreatment and catalytic oxidation post-treatment coupled with ABMBR for landfill leachate treatment, Sci. Total Environ. 794 (2021) 148557.
[44] C. Zhang, S. Li, H. Sun, S. Fu, J. Jingjing, H. Cui, D. Zhou, Feasibility of intimately coupled CaO-catalytic-ozonation and bio-contact oxidation reactor for heavy metal and color removal and deep mineralization of refractory organics in actual coking wastewater, Bioresour. Technol. 408 (2024) 131154.
[45] B. Zhou, X. Zhang, P. Wang, X. Zhang, C. Wei, Y. Wang, G. Wen, Catalytic performance and insight into the mechanism of CeO2 nanorod catalysts in phenol ozone oxidation reaction, Ceram. Int. 50 (2024) 394–402.